Blended Blown Flaps and Vectored Thrust for Low-Speed Flight

John E. Carr*
Grumman Aerospace Corporation, Bethpage, New York

Short take-off and landing (STOL) capability is a recurring design goal for current and future aircraft design studies to meet reduced field length requirements, provide increased stores "bring back" capability, enhance carrier aircraft payload launch and recovery envelopes, and improve in-flight maneuvering. The Grumman Corporation has conducted a study to design and build an A-6 STOL demonstrator aircraft for the Navy that employes two-dimensional vectored nozzles and chordwise blowing for low-speed flight. If completed, this program would demonstrate operationally acceptable STOL performance with minimum loss in cruise performance. The results of a two-dimensional airfoil test determined that a plain blown flap with a large-radius, upper leading-edge blowing segment and a conventional-shaped trailing-edge section had better high-lift capability for the available blowing momentum of the design. Extensive three-dimensional wind tunnel testing verified predicted longitudinal characteristics, showed acceptable longitudinal and lateral-directional control, and defined design limitations associated with the high-lift system.

Nomenclature

c',c	= 2- and 3-D aerodynamic chord, respectively; ft
C_d,C_D	= 2- and 3-D drag coefficients, respectively
C_{D0}	= minimum drag
C_ℓ,C_L	= 2- and 3-D lift coefficients, respectively
C_l,C_m	= 3-D rolling-and pitching-moment coefficients, respectively
C_{n_β}	= yawing-moment derivative
C_n	= 3-D yawing-moment coefficient
C_T	= thrust coefficient, gross thrust/qS
C_μ	= blowing-momentum coefficient, $\dot{m}V_j/qs$
i_{HT}	= incidence of horizontal tail
$\dot{m}$	= mass flow through blowing slot, slug/s
q	= dynamic pressure ratio, psf
R	= trailing-edge radius
V	= aircraft velocity, knots
V_j	= jet velocity, ft/s
V_{stall}	= aircraft velocity where wing stalls
2-D,3-D	= 2- and 3-D data or test, respectively
α	= angle of attack
β	= angle of sidelip
δ_e	= elevator deflection angle
δ_{FL},δ_N	= flap and nozzle deflection angles, respectively
δ_{SL}	= leading-edge slat deflection

Introduction

SHORT takeoff and landing (STOL) capability is a recurring design requirement of current and future aircraft development programs. STOL technology can provide forward-base operational capability from shortened and undeveloped airfields. Carrier operations can also be improved by larger store and fuel "bring back" capability combined with enlarged launch and recovery envelopes. The current environment of ever-increasing mission weight requirements to counter and deliver sophisticated airborne weaponry practically dictates going beyond purely aerodynamic high-lift systems. Yet practical demonstration of STOL technologies is limited to a few demononstrator aircraft, with little attention to fleet operational requirements or the design and development of flight control standards for naval STOL operation.

This paper documents aerodynamic concerns of an A-6 STOL Demonstrator study[1] conducted by the Grumman Corporation. The flight vehicle, illustrated in Fig. 1, is designed to blend an existing operational airframe with a modern engine design with two-dimensional (2-D) vectored nozzles, and chordwise trailing-edge blowing. This flight vehicle would demonstrate operationally acceptable STOL and cruise performance and allow investigation and development of innovative flight controls methodology for future STOL aircraft design. Analysis has indicated that this combination would reduce takeoff and approach speeds by 20%, with a corresponding takeoff and landing ground roll reduction exceeding 40%. Similar improvement in carrier wind-over-deck requirements and carrier operating weights is possible. This would provide naval STOL performance and increase the mission capability of the original design.

Discussion

Concept Development

The A-6/Circulation Control Wing (CCW),[2] a successful Navy STOL program built and tested by Grumman under contract to David W. Taylor Naval Ship Research and Development Center (DTNSRDC), used high-pressure engine bleed air blown tangentially in a thin jet over a cylindrical Coanda trailing edge to generate trimmed lift coefficients up to 3.9. Controlled flight was demonstrated down to speeds of 67 knots, and takeoff and landing ground roll reductions of 30 and 50% were demonstrated.[3] However, the A-6/CCW Demonstrator was design-limited to low-speed flight demonstration. Investigative work continued at Grumman and elsewhere to exploit the technology of CCW without penalizing high-speed performance.

The ADEN program and many other recent nozzle design studies have shown the benefits that can be gained with 2-D vectored nozzles. Overall aircraft performance can be enhanced through proper incorporation of a 2-D nozzle into the design[4,5] Lift gain from vectored thrust can be maximized by placing the thrust vector close to the c.g., and

Presented as Paper 84-2199 at the AIAA 2nd Applied Aerodynamics Conference, Seattle, WA, Aug. 21-23, 1984; submitted Nov. 17, 1984; revision submitted July 23, 1985.

*Senior Aerodynamics Engineer. Member AIAA.

reducing the trim penalty from the associated moment. Placement of the nozzle near the wing trailing edge also provides jet-induced lift on the wing. This type of installation is possible on the A-6 airframe and promises a significant decrease in takeoff and landing approach speeds.

Development of blown flaps that exploit the Coanda effect of a fluid passing over a curved surface to generate lift continued at both Grumman and DTNSRDC.[6,7] The Coanda-type flaps ranged from very small circular flaps of 0.45% chord radius, to dual-radius flaps of various chord ratios, to a 23% chord plain blown flap. This type of flap used a high momentum jet to energize the surrounding fluid, maintaining attached flow to larger deflections than a conventional flap. The result is a substantial increase in induced lift (boundary-layer control and supercirculation). The DTNSRDC designs were intended to exploit the large jet momentum associated with C_μ values greater than 0.1, where supercirculation provides significant lift enhancement. These included the small- and dual-radius flaps. The Grumman designs were intended to use less momentum, $C_\mu < 0.05$; provide good lift enhancement at $C_\mu = 0$; and impose no cruise drag penalty on the design. A joint DTNSRDC/Grumman 2-D wind tunnel test was conducted to evaluate all of these designs. The results indicated superior lift enhancement with the dual-radius flap at high C_μ values, however, the larger chord plain blown flap generated more lift for C_μ values, below 0.05.

Design Considerations

A design study of lift enhancement with vectored thrust (TV) and CCW revealed that certain disadvantages of either system alone could be minimized by combining both technologies into a common design. This could be demonstrated on an A-6 airframe where both technologies can be accommodated conveniently. The resulting system would not only be better than TV and CCW alone, but the combination would interact favorably.

True CCW requires a large amount of high momentum air. Several studies, including the A-6/CCW have shown that while lift is favorably enhanced, several less desirable characteristics also appear. The large supercirculation of CCW produces a large nose-down pitching moment. Trimming this with a conventional horizontal stabilizer located aft of the c.g. reduces the net lift gained. Downwash behind the flap can also be considerable for high C_μ. This may drive the design of the horizontal stabilizer into a configuration unreasonable for cruise, as on the A-6/CCW. Leading-edge treatments may be required to prevent early departure, which would reduce the useable C_L of the system. Such devices increase weight and may induce cruise drag penalties. The large amount of bleed air required for high C_μ values may either significantly reduce available engine thrust for forward flight or require a heavy and thirsty auxiliary unit. Large increases in drag also accompany large C_μs and may limit acceleration capability. Duct size is determined by maximum bleed air requirements. If the duct diameter required to achieve the proper flow cannot be retained in the existing airfoil and airframe contours, significant cruise drag and weight penalties may be incurred. Adverse lateral-directional effects have been found with large blowing momentums.

Fortunately the largest portion of the induced lift is achieved at relatively low C_μ values, while the less favorable effects previously mentioned are not yet critical. This was the design philosophy behind the acceptance of a low amount of engine bleed air, available from the design engine. Relatively low momenum bleed air would provide C_μs less than 0.05. This would reduce the maximum induced lift, slightly. However, it would require less trim lift, smaller duct size, and no leading-edge treatment. This would also produce less high-lift drag and downwash, resulting in a simpler and lighter aerodynamic design. The high-lift system would be enhanced by vectored thrust.

Incorporating vectored thrust on the A-6 also requires some design compromises; studies have shown severe downwash. Adverse lateral-directional characteristics can accompany a midfuselage nozzle, aft-tail design. Also, high thrust deflections, while providing large lift enhancement, reduce the thrust component available for forward flight. The required design must provide high lift with favorable aircraft performance.

The original A-6 design incorporated a tilting tailpipe to provide thrust vectoring. Vectored thrust was recognized as a means to reduce takeoff and landing speeds with powered lift. However, the limited thrust-vectoring capability and low wing loading of the design provided limited performance improvement. This, and the weight penalties associated with the tilting tailpipe, led to its removal.

The A-6 STOL 2-D nozzle design provides vectoring capability between 4 and 60 deg, compared to 30 deg for the A-6 tilting tailpipe. The 2-D nozzle is lighter and allows optimization of the thrust-vector angle for cruise, takeoff, and landing. The thrust vector can be set to optimize cruise performance by reducing thrust requirements for 1-*g* flight. A takeoff thrust vector of 35 deg provides direct-powered lift while meeting acceleration requirements at lift-off. The thrust required on approach is low relative to the thrust available; a thrust vector of 60 deg maintains the glide slope and permits excess available thrust to be used for direct-powered lift.

Thrust vectoring poses a practical problem neatly handled by the A-6 aircraft. The thrust vector, aft of the c.g. in a majority of designs, generates a large nose-down pitching moment. This must be balanced by an opposing moment to maintain aircraft attitude or to rotate the aircraft for lift-off. The farther aft the thrust vector from the c.g., the larger the moment to be balanced. For the A-6, the engine tailpipe is located at the wing trailing edge relatively close to the c.g. The horizontal tail surface is located well aft of the c.g. and provides a significant tail arm to balance the thrust moment. Thrust vectoring also produces downwash behind the jet. In the case of the A-6, the increased downwash, which accompanies increased jet deflection, increases the lift on the horizontal tail and effectively reduces the nose-down moment remaining to be trimmed.

These two powered-lift systems provide significant performance improvement at the current A-6 operational wing loadings. Figure 2 illustrates the improvement in lift, expressed as C_L and approach speed achieved with boundary-layer control and thrust vectoring combined and individually, compared to the A-6 high-lift system. For a constant $\dot{m}V_j$ lift enhancement due to BLC increases with decreasing velocity, while the direct lift from thrust vectoring remains independent of aircraft velocity. In terms of C_L, for constant blowing momentum, BLC provides a larger increment when combined with thrust vectoring than is achieved with BLC alone.

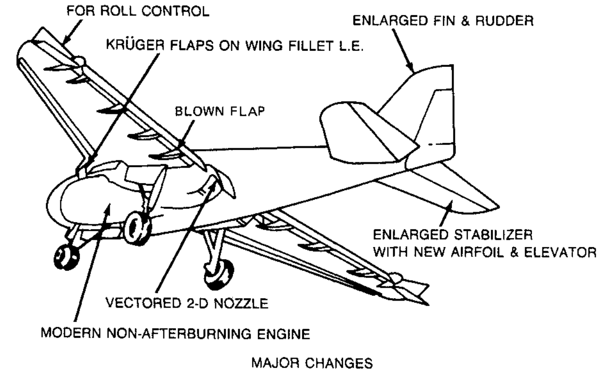

Fig. 1 A-6 STOL demonstrator.

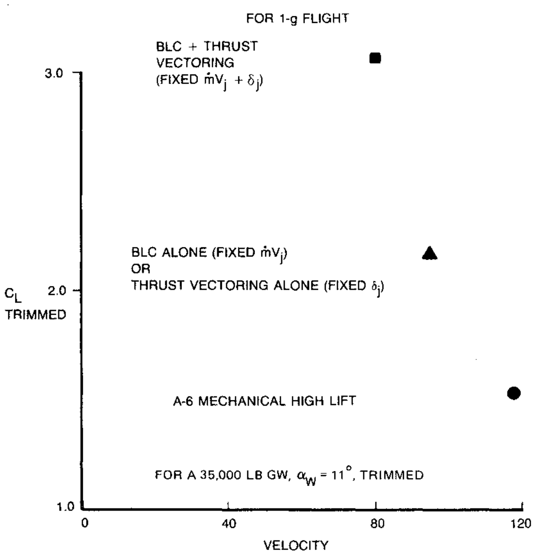

Fig. 2 High-lift improvement in C_L and velocity.

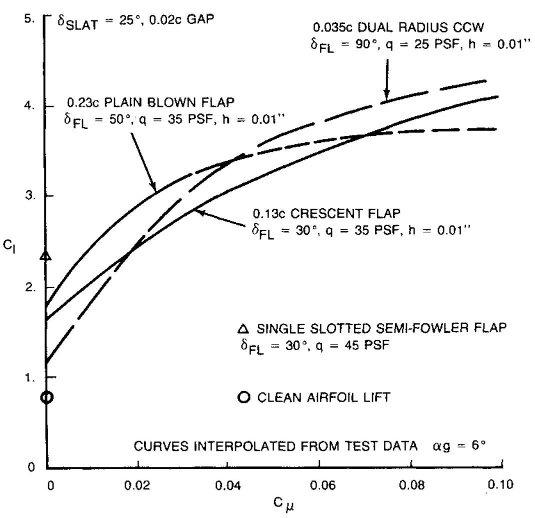

Fig. 3 2-D lift comparison, BLC on.

2-D Blown Flap Evaluation

Two Grumman-designed blown flaps utilizing the Coanda principle to optimize lift were tested on a 2×3-ft 2-D model of the NACA 64A008.4 MOD A-6 airfoil section, a 23% chord plain blown flap (PBF) with a large Coanda surface as a leading edge and a conventional-shaped trailing edge, and a 13% chord crescent flap with a circular upper surface, representing a retractable Coanda surface.

The 2-D wind tunnel test results indicated that the optimum flap design is dependent on the available C_μ range, not simply on maximum lift. A comparison of the BLC lift vs C_μ for the two flap candidates and a DTNSRDC 0.035c' dual-radius flap[7] is shown in Fig. 3. The 23%c' PBF achieves more lift than the 13% crescent blown flap at $C_\mu < 0.07$. Both designs show healthy BLC-off lift, due to the camber provided by the deflected flap, and compare well to the conventional flap lift. The clean airfoil lift and lift with a single-slotted semi-Fowler flap, $\delta_{FL} = 30$ deg, are also shown in Fig. 3. Good high-lift capability BLC off also was a requirement of the design. The 0.035c' dual-radius flap shows good BLC lift characteristics—generating more lift than the PBF at C_μ above 0.04, despite significantly lower BLC-offlift. The PBF, however, provides higher lift over most of the A-6 STOL 2-D C_μ range

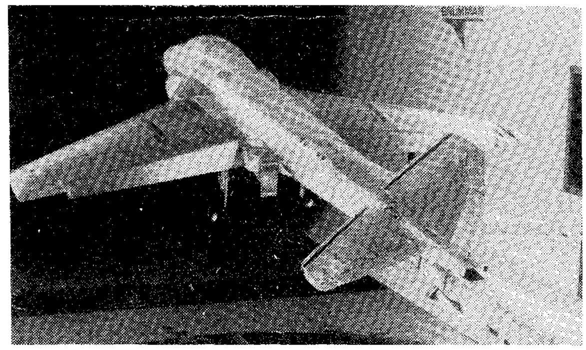

Fig. 4 A-6 STOL 1/8.5-scale wind tunnel model.

of 0 to 0.06 and higher lift BLC off, making it the logical choice. The available C_μ range must double before the crescent flap could provide significant improvement over the PBF.

3-D Wind Tunnel Test

Extensive wind tunnel testing was conducted on a powered 1/8.5-scale model of the A-6 STOL Demonstrator aircraft (Fig. 4). The testing determined basic lift and drag of the configuration and defined certain unknown effects of vectored thrust and chordwise blowing on lift, drag, longitudinal trim, and lateral-directional characteristics. Previous studies had indicated many of the effects to be highly configuration-dependent.

Basic configuration differences between the A-6E and A-6 STOL are enlarged horizontal and vertical tails to handle the lower flight speeds and downwash, 23%, chord blown flap, BLC in the wing, a Krueger flap on the glove leading edge, and 2-D vectored nozzles. The horizontal tail had a 0.3c elevator with 3:1 gearing at the maximum tail incidence, chosen based on test results.

Model forces and moments were recorded on a six-component balance system located in the model fuselage cavity. Pressures also were recorded on the wing and horizontal tail. Thrust simulation was achieved by high-pressure air exhausted through simulated 2-D nozzles located near the wing-root trailing edge. Flap blowing was achieved by pressuring a plenum located in the wing and exhausting it through a thin spanwise slot located forward of the flap leading edge.

3-D Test Results

Wind tunnel test results essentially verified predicted aerodynamic characteristics. Lift and drag data were close to prior estimates based on A-6 CCW data. Some limitations were found in longitudinal trim at very-low-speed conditions. BLC and deflected jets had minor effects on lateral-directional characteristics. However, the ground effects were considerable. The Krüger flap used on the wing glove leading edge provided protection from early stall at high C_μ, yet the A-6 leading-edge slat and wing glove appeared adequate for the desired C_μ range.

Lift

The A-6 STOL Demonstrator relies on a mechanical flap, BLC, deflected jets, and their interactions for high lift. Contributions of each element, individually and combined, are shown in Fig. 5. The thrust-included data shown illustrate total system lift, while the thrust-removed data reveal induced lift due to deflected jets. All data shown are for model scale.

Using this data and an approach angle of attack of 11 deg, lift coefficient increases from 1.35 to 2.17 due to BLC with a $C_\mu = 0.05$ and to 2.45 with thrust, $C_T = 1.0$, deflected 60 deg. BLC plus deflected thrust produce a power-on C_L of 3.32. The thrust-removed data indicate thrust-induced lift on the order of $\Delta C_L = 0.2$, including downwash on the horizontal tail. The increment due to thrust-induced lift alone must be measured

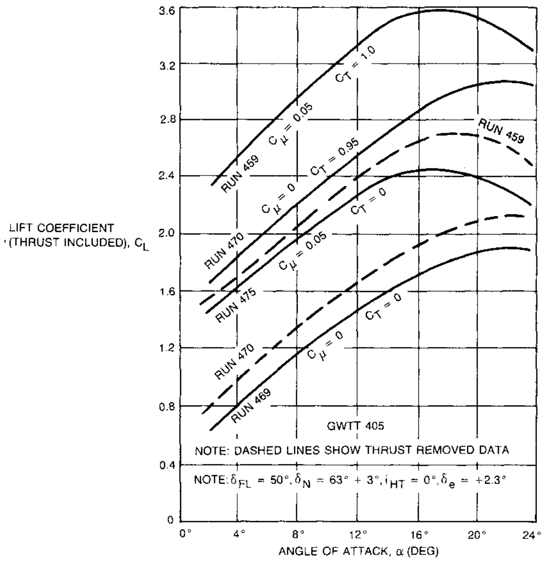

Fig. 5 Effect of C_μ and C_T on lift.

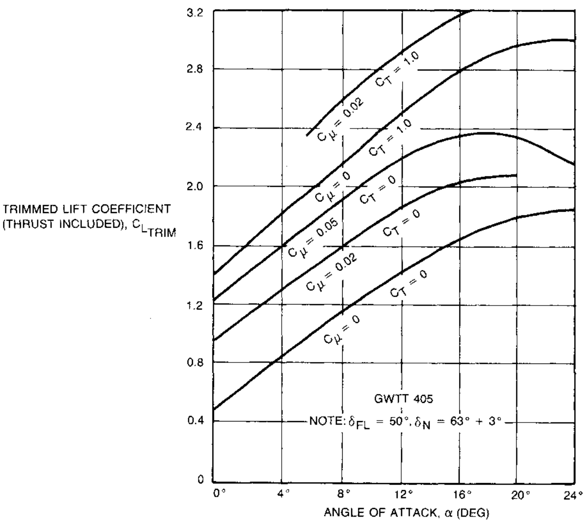

Fig. 6 Trimmed C_L.

tail-off; however, total lift including downwash on the tail is the important criterion. Thrust-induced lift is further reduced as a trimmed value. The aircraft relationship between C_μ and C_T is dependent on the available bleed air, engine thrust, and flight conditions. Approach criteria are determined by more than the C_L available. This comparison serves only to illustrate the effectiveness of the system.

Trimmed lift curves are necessary to evaluate the system. Downwash on the horizontal tail is different for each untrimmed curve shown in Fig. 5, as is the pitching moment due to lift. Trimmed lift curves are shown in Fig. 6. The model pitching moment at a $C_T = 1.0$, $C_\mu = 0.05$ condition could not be trimmed by the existing horizontal tail due to severe downwash. This does not limit the design since the condition exists only at flight speeds below 70 knots, which are outside of the design flight envelope. The problem may also be relieved by the full-scale Reynolds number. This does show how BLC can impose control limitations, however.

A comparison of 1-g flight speeds using total C_L from Fig. 6 illustrates the STOL capability of the powered lift system. All comparisons are for a 35,000-lb airplane at $\alpha = 11$ deg and sea level, standard day conditions. The power-off C_L requires a flight speed of 121 knots. BLC with $C_\mu = 0.02$ reduced this to

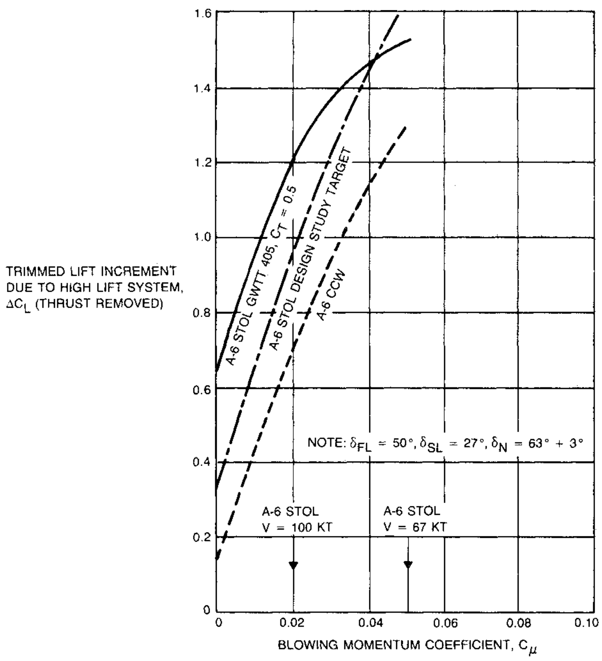

Fig. 7 High-lift system ΔC_L.

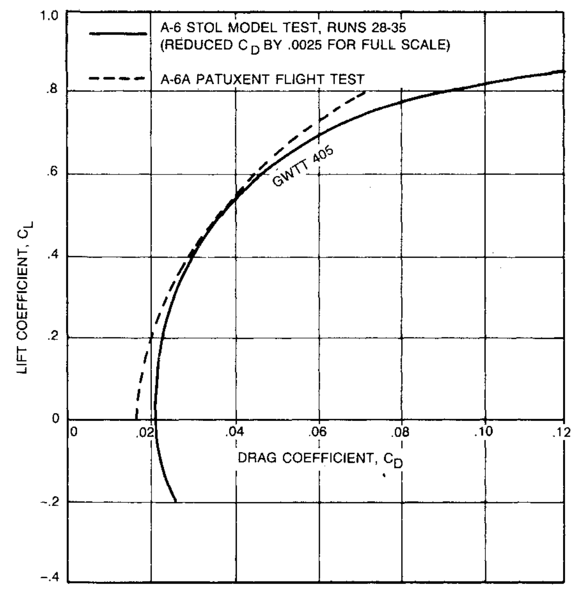

Fig. 8 Comparison of clean trimmed polars, A-6 and A-6 STOL, power off.

105 knots; deflected jets with $\delta_j = 61$ deg and $C_T = 1.0$ reduce this to 90 knots; and BLC plus deflected jets require only 83 knots. This represents a 30% reduction in speed, and a significant increase in STOL capability and aircraft safety. Comparisons are made at a constant angle of attack as opposed to standard safety margins common to conventional lift airplanes due to the nature of STOL aircraft.

A conventional aircraft with an approach speed of 120 knots would have a stall speed of approximately 100 knots, providing a 20% stall safety margin. This roughly corresponds to C_L stall of 1.95 and a C_L approach of 1.35. A STOL airplane having a C_L stall of 2.5 would have a stall speed of 88 knots. A 20% safety margin would yield a 106-knot approach speed, or a C_L approach of 1.74, a far larger margin than is reasonable. Carried to an extreme, the 20% margin would result in negative approach angle of attack for some high-powered STOL aircraft. STOL effects would be negated. The

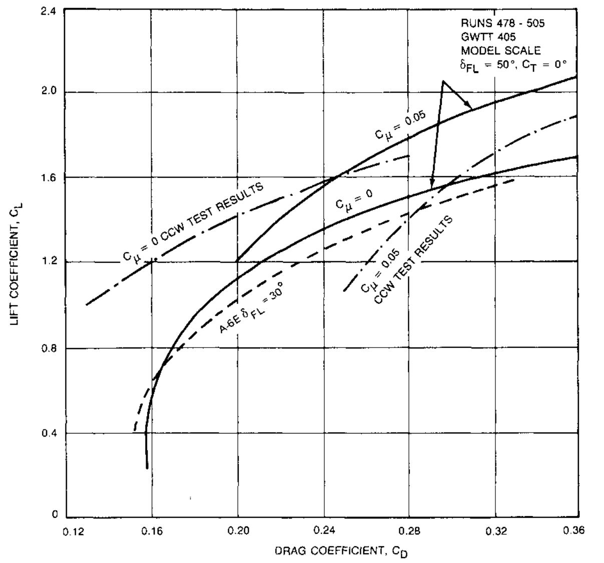

Fig. 9 High-lift trimmed polars A-6E, A-6 CCW, and A-6 STOL.

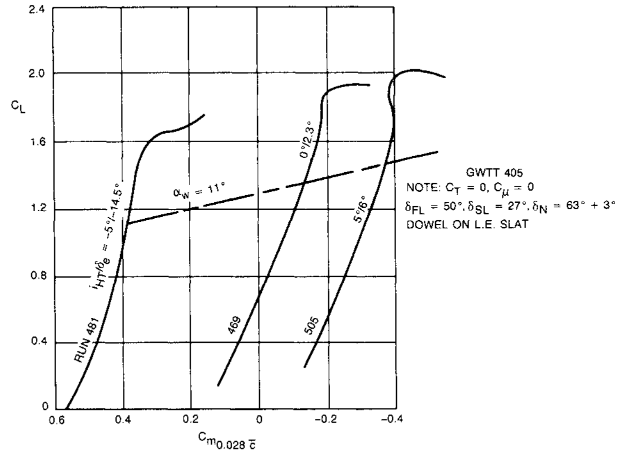

Fig. 10 Horizontal tail power, $C_\mu = 0$ and $C_T = 0.0$.

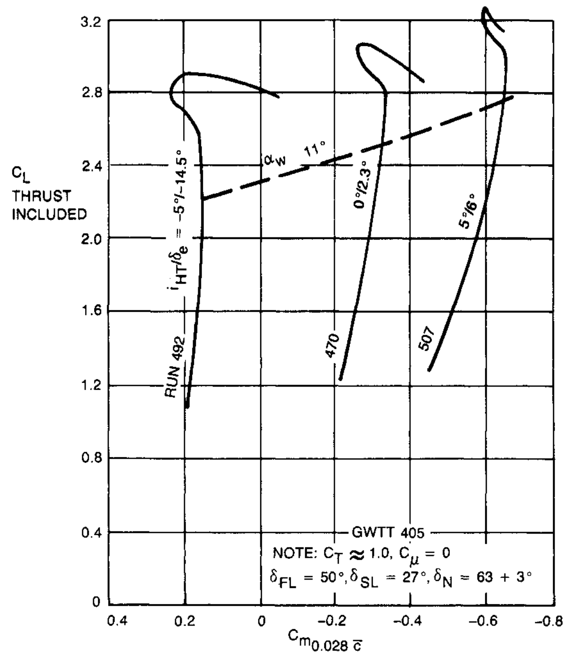

Fig. 11 Horizontal tail power, $C_\mu = 0$ and $C_T = 1.0$.

large C_L and low velocity associated with STOL aircraft require a different type of safety margin. A safety margin of 10-deg angle of attack roughly corresponds to the conventional safety margin of 1.2 V_{stall} for non-STOL aircraft and provides an adequate margin and reasonable approach speed for STOL aircraft. A stall angle of 21 deg is reasonable for the full-scale airplane, BLC on, which gives a STOL approach angle of attack of 11 deg and corresponds roughly to the current A-6 approach angle of attack.

The lift increment due to the high-lift system, thrust removed, exceeded predictions, as shown in Fig. 7. This was due in part to the lifting ability of the modified flap, BLC off, which nearly matches the A-6E 30% chord single-slotted flap, and to the increment in thrust-induced lift. The 23% cord PBF shows a declining increase in lift at C_μ above 0.03. The same effect was seen in the 2-D test results. Since the A-6 STOL Demonstrator is limited to C_μ below 0.05, this phenomenon is not significant. However, if more blowing momentum were available, consideration of a different type of blown flap would be required. The aircraft velocity corresponding to C_μ values of 0.02 and 0.05 are shown in Fig. 7 for sea level, standard day conditions. The useful powered-lift speed range for the A-6 STOL is between 80 and 90 knots.

Drag

The A-6 STOL Demonstrator was designed to provide adequate high lift with as little increase in cruise drag as possible. Figure 8 compares the clean (flaps up; gear and slats retracted) drag from the test with an A-6A Patuxent River flight-test polar. Test data were corrected for excrescence drag and full-scale effects by subtracting a $\Delta C_D = 0.0025$. Any drag increase is due primarily to modifications required to accommodate the new engine installation.

The high-lift drag in Fig. 9 is similarly close to the A-6E flight test high-lift drag polar with $\delta_{FL} = 30$ deg, as shown. Also shown is a comparison with the A-6/CCW wind tunnel data. The A-6/CCW data shows lower drag BLC-off due to the lack of a flap. Unlike cruise—where drag is a penalty—drag is beneficial in landing because it allows a higher thrust setting, providing greater direct lift, induced lift, and better wave-off capability due to lessened spool-up time to achieve full thrust. The effect of BLC on drag varied for the A-6 STOL and CCW. The CCW had an increase in drag at $C_\mu = 0.05$ at a constant C_L; at the same conditions, A-6 STOL shows a reduction in C_D. The thrust component of C_μ is one possible explanation. For the CCW, deflection of the BLC jet is high; while for the A-6 STOL, the jet follows the flap creating a lower deflection and net drag reduction. Overall drag was not significantly higher than the A-6E, and should pose no design problems.

Longitudinal Trim and Static Stability

Longitudinal control is provided by a large horizontal tail with a supercritical airfoil section and a 30% chord elevator geared 3:1. This was selected in recognition of the high downwash normally associated with deflected jets. This downwash is evidenced in the design as a decrease in static stability and, at certain conditions, an inability to trim the airplane. Figure 10 shows good stability and good elevator authority for the power-off condition. However, in Fig. 11, at $C_T = 1.0$ with jets defected 60 deg, static stability is decreased significantly and elevator authority is reduced. The addition of BLC (Fig. 12) increases static stability for $i_{HT} = 5$ and 0 deg, but the additional downwash at $C_\mu = 0.02$ stalls the horizontal tail at a low α. Higher values of C_T and C_μ completely stalled the tail and, in some cases, were untrimmable. This could require a speed limitation on the design. However, areas of concern were not in the useful flight envelope. The tail stall may be relieved at full-scale Reynolds numbers where the $C_{L\max}$ of the tail section is significantly higher than at test conditions.

A summary of the effects of BLC and thrust on static stability is provided in Fig. 13. With $C_T = 0$ and c.g. referred to 0.28c, the aircraft has good static stability power-

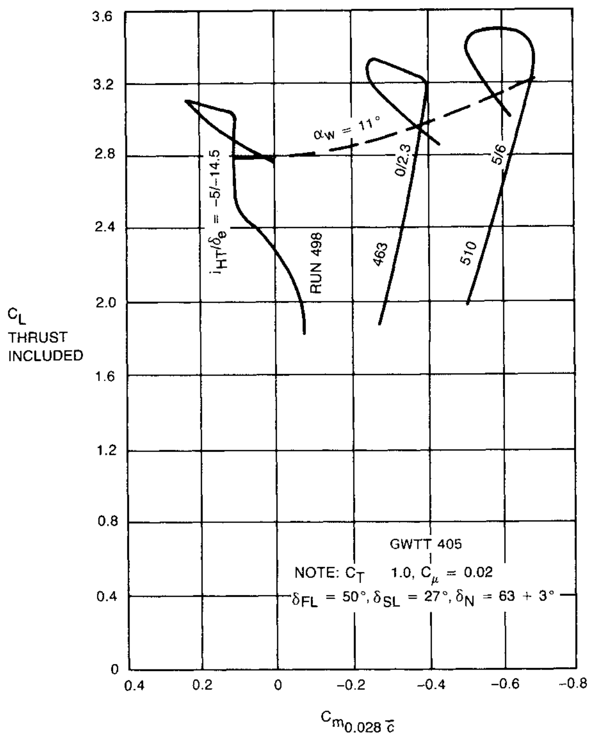

Fig. 12 Horizontal tail power, $C_\mu = 0.02$ and $C_T = 1.0$.

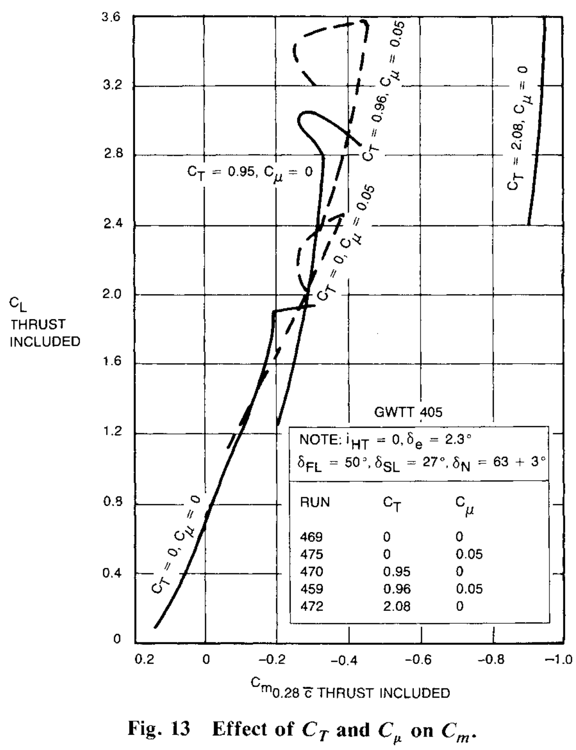

Fig. 13 Effect of C_T and C_μ on C_m.

off—increased with the addition of BLC, $C_\mu = 0.05$. Power significantly reduces static stability, as shown by the $C_T = 0.95$, $C_\mu = 0$ and $C_T = 2.08$, $C_\mu = 0$ curves—almost becoming neutral. Again, addition of BLC, $C_T = 0.96$, $C_\mu = 0.05$ restores some static stability. Note also that the increment in C_m is not strictly thrust times arm as it would be tail-off. Downwash on the tail increases the tail C_L, countering the thrust moment. Thus, the change in nose-down pitching moment due to jet deflection is somewhat compensated for by the change in downwash due to the jet. This reduces the stick motion required to trim nozzle transition and changes in thrust.

Lateral-Directional Findings

BLC and vectored thrust did not adversely affect lateral-directional characteristics. Spoiler effectiveness was less for the A-6 STOL BLC-off than the A-6E, however, with BLC on, spoiler effectiveness is increased considerably. Sufficient rudder power was found to handle all single-engine-out conditions. Directional static stability was increased with power.

Ground Effects

The influence of the ground on BLC and vectored thrust was found to be considerable. Unfortunately, no final test data for this condition were available. However, severe distortion of the longitudinal characteristics and severe suck-down were observed during testing at high vector-high C_T conditions.

Conclusion

Use of thrust vectoring combined with chordwise blowing appears to be a viable STOL concept. Results of tests discussed herein confirm the viability of the A-6 STOL Demonstrator and support predicted aerodynamic characteristics. Reductions in takeoff and approach speeds exceeding 20%—and in ground distances 40% calculated with the predicted aerodynamic characteristics can be verified with the test results.

Results of the two-dimensional (2-D) testing illustrated the need to consider several criteria in the flap selection and determined selection of a 23% chord plain blown flap for the levels of wing blowing in this design.

The 3-D wind tunnel test data either matched or improved upon the estimated data used during the design study and provided information concerning effects and interactions of chordwise blowing and thrust vectoring. Some minor limitations in application of the described high-lift system became apparent. The data shows a loss in longitudinal stability and horizontal tail authority with high nozzle deflection at high C_T and C_μ conditions. These conditions exist only below 80 knots, which is considered outside the useful flight envelope of the design. Apparent limitations did not impact predicted performance. Higher Reynolds number conditions for full-scale aircraft may alleviate most conditions imposing limitations. This could be verified either with a wind tunnel test nearer a full-scale Reynolds number or during a flight-test phase of demonstrator development.

Acknowledgments

The author wishes to acknowledge the participation and support of Vladimir Seredinsky, Technical Specialist, Grumman Aerospace Corporation, and Robert J. Englar, DTNSRDC, in the tests detailed in this paper.

References

[1]Carr, J.E., "Aerodynamic Characteristics of a Configuration with Blown Flaps and Vectored Thrust for Low-Speed Flight," AIAA Paper 84-2199, Aug. 1984.

[2]Englar, R.J. el al., "Design of the Circulation Control Wing STOL Demonstrator Aircraft," *Journal of Aircraft*, Vol. 18, Jan. 1981, pp. 51-58.

[3]Pugliese, A.J. and Englar, R.J., "Flight Testing the Circulation Control Wing," AIAA Paper 79-1791, Aug. 1979.

[4]Doonan, J.G. and Callahan, C.S., "A High Speed Wind Tunnel Test Evaluation of STOL Dedicated Advanced Exhaust Nozzle Concepts," AIAA Paper 83-1225, June 1983.

[5]Landfield, J.P., "STOL Technology for Conventional Flight Enhancement," AIAA Paper 84-2397, Oct. 1984.

[6]Englar, R.J., "Development of an Advanced No-Moving-Parts High-Lift Airfoil," Paper ICAS-82-6.5.4, *Proceedings of ICAS/AIAA Aircraft Systems and Technology Conference*, Seattle, WA, Aug. 1982.

[7]Englar, R.J. and Huson, G.G., "Development of Advanced Circulation Control Wing High Lift Airfoils," AIAA Paper 83-1847, July 1983; also, Rept. DTNSRDC-83/109, Dec. 1983.